Modelling X-ray or neutron scattering spectra of lyotropic lamellar phases : interplay between form and structure factors

F. Nallet, R. Laversanne, D. Roux

Classification
Physics Abstracts
61.10D — 61.30E — 82.70

Modelling X-ray or neutron scattering spectra of lyotropic lamellar phases : interplay between form and structure factors

F. Nallet, R. Laversanne and D. Roux

Centre de recherche Paul-Pascal, CNRS, avenue du Docteur-Schweitzer, F-33600 Pessac, France

(*Received 4 August 1992, revised 18 December 1992, accepted 6 January 1993*)

Abstract. — The lamellar phase of two binary systems, AOT/water and DDAB/water, is studied by X-ray or neutron scattering techniques, along dilution lines. We observe on both systems a large wave vector diffuse scattering with the following features : i) its *shape* is independent of dilution ; ii) its *intensity* scales linearly with the bilayer volume fraction ; iii) it is *sensitive* to the scattering length density profile of the amphiphilic bilayer. With the help of a model combining geometry of the bilayers and layer displacement fluctuations, we quantitatively describe our data. This allows us to ascribe the diffuse scattering to the *strongly enhanced* thermal diffuse scattering which originates in the Landau-Peierls instability characteristic of the smectic A symmetry of our systems. The model has two important consequences : i) the form factor of the amphiphilic bilayer may be extracted from the large wave vector diffuse scattering ; ii) the Bragg peak intensities, modulated by the bilayer form factor, also depend on the amplitude of the thermally-excited elastic waves, i.e. on the magnitude of the elastic constants.

Introduction.

An interesting variety of structures and behaviours are encountered in the study of the surfactant/solvent systems also known as lyotropic phases. In many cases the building unit has locally the shape of a *membrane*, i.e. a planar bilayer of surfactant molecules. Examples of such structures, with different long-range or internal symmetries are, for instance lamellar (L_α) or cubic phases and « sponge » (L_3) or vesicle phases [1-5]. The membranar nature of the building units is often established through a determination of the form factor, using radiation (X-ray, neutron) scattering. The form factor may be directly seen in the high wave vector part of the scattered spectrum, for disordered structures [e.g. 2, 3] or indirectly reconstructed from the height modulation of the Bragg peaks arising in long-range-ordered lamellar [4] or cubic [5] structures. Another method yet is routinely used for the measurement of the form factor of the building unit in *one-dimensionally-ordered* structures : it takes advantage of the (usually strong) diffuse scattering present in such systems [6], arising from displacement fluctuations about the ideal lattice positions. These fluctuations are often described in purely geometric terms, as a so-called « stacking disorder » [6, 7], but their thermal origin, especially in the vicinity of phase transitions between differently ordered structures is mentioned [8]. In this paper, we reconsider the interpretation regarding the diffuse scattering in one-dimensionally-

ordered systems : we show that the thermally-induced layer displacement fluctuations in lamellar (smectic A) phases, ultimately controlled by the magnitude of the elastic constants of the smectic structure, account *quantitatively* for the Bragg and diffuse components of the scattering. As a consequence, the product $\bar{B}$. K of two elastic constants may be measured from the spectra, in addition to the usual structural parameters.

We first present our X-ray and neutron scattering results on two lyotropic lamellar phases. Besides the Bragg scattering, with a form factor modulation of the peak heights, our results also display a significant diffuse scattering at large wave vectors. Then, we quantitatively interpret the Bragg and diffuse components of the scattering with a model of the lamellar phase that takes into account both membrane geometry and the thermodynamic origin of the layer displacement fluctuations. This results in : i) bilayer form factor parameters, as in recent works on the same or similar systems [9, 10] ; ii) elastic constant estimates. The generalization of our model to other weakly bound structures with long-range translational order could open new perspectives for the determination of both form factors and elastic constants.

Experimental results.

We have studied the lamellar phases of two binary surfactant/solvent systems : AOT/water (AOT is bis 2-ethylhexyl sodium sulphosuccinate) and DDAB/water (DDAB is didodecyl dimethyl ammonium bromide). The AOT surfactant has been used as received (Sigma Corp ; purity 99 %) ; DDAB was synthesized (dimethyldodecyl amine alkylation in lauryl bromide) and purified (two recrystallizations in ethyl acetate and one in ether) in our laboratory. Surfactants have been mixed with Milli Q water (Waters Co.) or with heavy water (CEN-Saclay) in amounts chosen to get lamellar samples at room temperature, according to the phase diagrams of the AOT/water [11] or DDAB/water [10] systems. For X-ray experiments (on the AOT system only) samples are held in sealed thin-walled glass tubes (diameter $D = 1.5$ mm, thickness $e = 0.01$ mm). Spectra have been recorded on a home-made camera (copper rotating anode operating at 18 kW ; graphite monochromator set to the $\lambda = 1.54$ Å line ; collimation with slits ; scintillation detector with background $0.6\ s^{-1}$). Neutron spectra have been obtained with AOT/D_2O or DDAB/D_2O samples held in 1 or 2 mm quartz cells, at Laboratoire Léon-Brillouin (CEN-Saclay, France) on beam lines PAXE (AOT) or PAXY (DDAB). Both X-ray and neutron scattering experiments have been performed at room temperature. On the dilution line for the AOT system, the surfactant volume fraction ϕ ranges from $\phi = 0.60$ to $\phi = 0.14$; for neutron scattering experiments with DDAB, ϕ ranges from 0.08 to 0.03. Except the most concentrated AOT sample (with a transmission 0.48), all samples have transmissions in the range of 0.7, which ensures that double or multiple diffusion does not contribute significantly to the spectra.

The AOT neutron scattering spectra are displayed in figure 1. Bragg peaks are observed all along the dilution line. When present, second order reflections are observed at twice the wave vector of the first order ones, as expected for a smectic long-range order. The location of the first order peak q_0 moves towards small wave vector values according to the simple dilution law, $q_0 \propto \phi$, as the surfactant volume fraction ϕ is decreased. This classical behaviour is consistent with a simple geometric model of the lamellar phase, described as a periodic stack with period $d = 2\ \pi/q_0$ of planar membranes of thickness δ (see Fig. 2) which yields $q_0 = 2\ \pi\phi/\delta$. This « geometric » thickness, deduced from the neutron data is $\delta = 22$ Å.

More complex is the effect of dilution on the AOT X-ray spectra. First, as already noted long ago [12], there is an *intensity* anomaly for surfactant compositions ϕ in the range 32-44 %. It is apparent in figure 3 that the normalized height of the first order Bragg peak starts decreasing as ϕ decreases to become equal to the height of the second order Bragg peak at $\phi = 0.48$ (Fig. 3b) and even vanishes at $\phi = 0.38$ (Fig. 3d). At this latter concentration the first and only

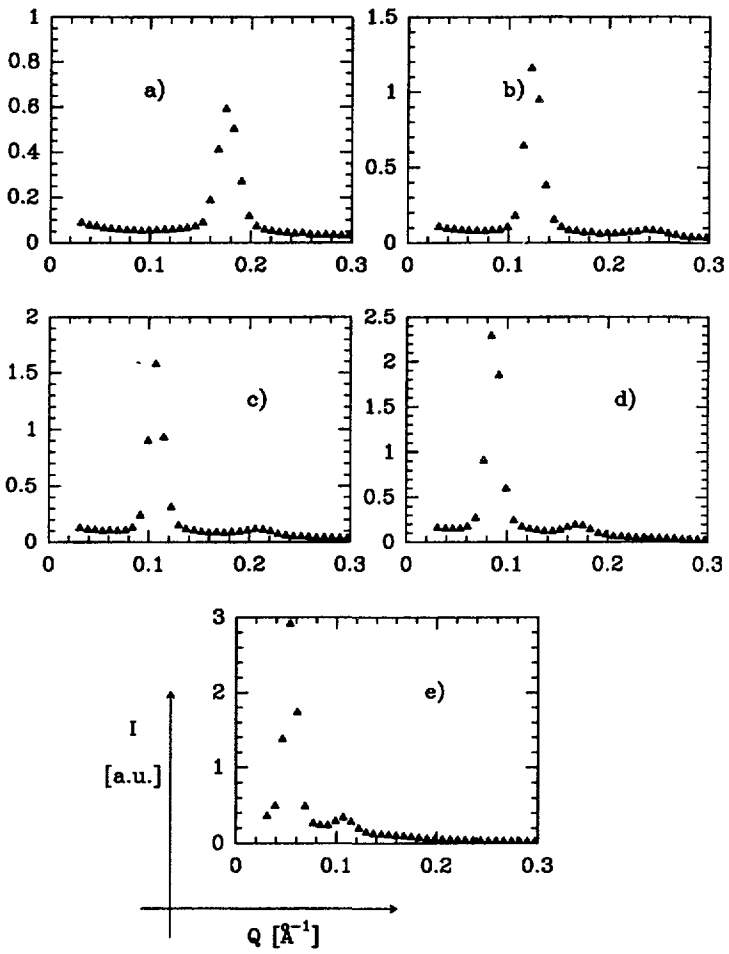

Fig. 1. — Intensity profiles in the neutron scattering experiment on AOT ; surfactant volume fractions, from a) to e) : 0.62, 0.43, 0.37, 0.30 and 0.18 ; the intensity units are arbitrary.

observable peak is therefore the *second order* peak. At lower concentrations ($\phi = 0.3$ and below) the first order peak reappears at the position expected from the simple dilution law. The membrane thickness we get is $\delta = 21$ Å ($\delta = 19.55$ Å in reference [12] ; differences in water content of the surfactant used could explain this discrepancy). The wave vector dependence of the normalized intensity of the first and second order X-ray Bragg peaks is plotted in figure 4. The vanishing of the peak height is clearly visible around $q = 0.12$ Å^{-1}.

Further, all the AOT X-ray spectra display in addition to the Bragg peaks a significant diffuse scattering, which appears as a broad hump in the intensity curves for wave vectors between $q \approx 0.1$ Å^{-1} and $q \approx 0.5$ Å^{-1} Such a signal is not observed on the neutron spectra (compare for instance Fig. 1e with Fig. 3e). The shape of the diffuse scattering does not vary appreciably along the dilution line. This is shown in figure 5 where the X-ray scattering data for three different AOT volume fractions have been superimposed in normalized units (intensities divided by the thickness, transmission and surfactant volume fraction of the samples). It is noteworthy that the small wave vector minimum in the diffuse scattering occurs at about $q = 0.12$ Å^{-1}, i.e. at the very position where the first order Bragg peak intensity vanishes.

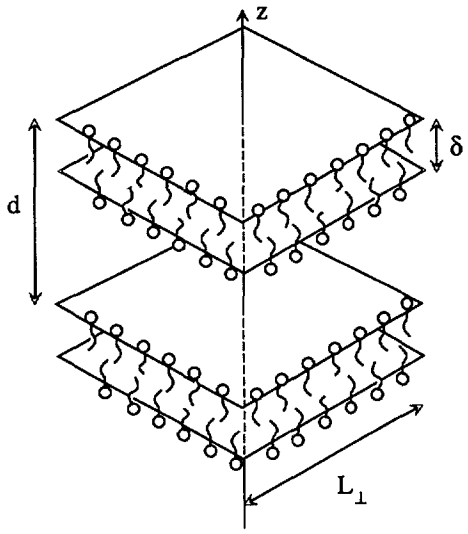

Fig. 2. — Geometrical model of a lyotropic lamellar L_α phase ; the planar surfactant bilayer has a thickness δ ; the bilayers are stacked along the direction z with a period d.

Similar observations on both peak intensities and diffuse scattering have been reported recently for an X-ray study of the lamellar phase of the (quasi) ternary AOT/decane/water + NaCl system [9]. Moreover, the large wave vector, diffuse component of the scattering was shown to be identical *in absolute units* for both lamellar and « sponge » samples built with the same oil-swollen surfactant bilayer, irrespective of dilution. This feature was ascribed to the form factor contribution to the scattered intensity [9]. It has been used in determining the scattering parameters of the bilayer in a cetyl pyridinium chloride/hexanol/water + NaCl lamellar phase [13].

In the following part, we extensively study a simplified, but still realistic model of the scattering by a lamellar phase and show how, through the interplay between Bragg and thermal-diffuse scattering that is introduced, it gives a complete, quantitative description of the previous observations.

Interpretation.

The intensity I_{id} of a radiation scattered at a wave vector $\mathbf{q}$ by an irradiated volume V of a sample characterized by a scattering length density $\rho(\mathbf{x})$ is classically given by :

$$I_{id}(\mathbf{q}) = \left\langle \left| \int_V \rho(\mathbf{x})\, e^{i\mathbf{q}\cdot\mathbf{x}}\, d^3\mathbf{x} \right|^2 \right\rangle \tag{1}$$

where $\langle .. \rangle$ denotes a thermal averaging of the enclosed expression (the effects of a finite resolution are momentarily ignored).

GEOMETRICAL MODELS. — Various models for the scattering length density $\rho(\mathbf{x})$ have been proposed, for the purpose of describing specific parts of the scattering spectrum of a lyotropic lamellar phase. For instance, the basic occurrence of peaks at regularly spaced Bragg positions $p \cdot q_0$ (p is an integer and q_0 the first order peak position in reciprocal space) stems from any scattering length density that is (perhaps only in some reference state) a one-dimensionally

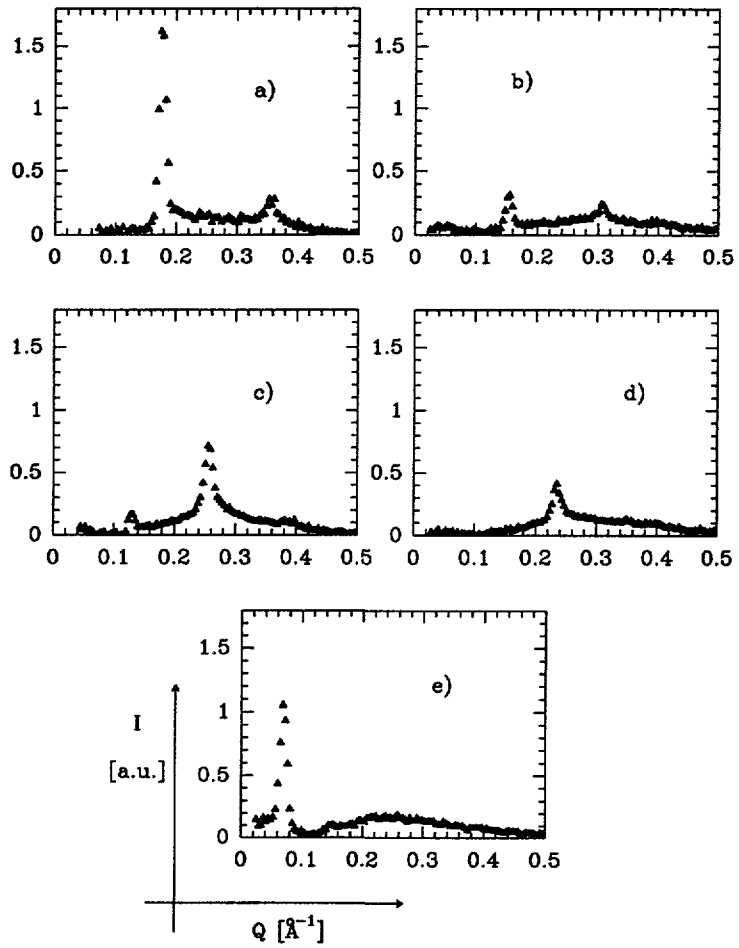

Fig. 3. — Intensity profiles (normalized by the thickness, transmission and membrane volume fraction of the samples) in the X-ray scattering experiment on AOT ; surfactant volume fractions from a) to e) : 0.59, 0.48, 0.43, 0.38, 0.24 ; note the disappearance of the first order Bragg peak at the surfactant volume fraction 0.38.

periodic function of period $d = 2\pi/q_0$, along a direction which we call z in the following. Furthermore, the commonly observed height modulation of successive Bragg peaks is usually ascribed to the form factor of the bilayer in the following, purely geometric way : a finite-size crystal of a lyotropic lamellar phase is described as the regular stacking — period d — along an axis z of N identical plaquettes-thickness δ ; lateral extension $L_\perp$ — all oriented normally to z (Fig. 2). The scattering length density is defined by :

$$\rho(\mathbf{x}) = \sum_{0}^{N-1} \rho_0(z - nd), \quad |\mathbf{x}_\perp| < L_\perp$$
$$\rho(\mathbf{x}) = 0, \quad \text{otherwise} \tag{2}$$

where $\rho_0(z)$, the scattering length density profile of one plaquette, has non-zero values only when $0 \leqslant z \leqslant \delta$. One then easily shows from equation (1) that the height of the Bragg peak of

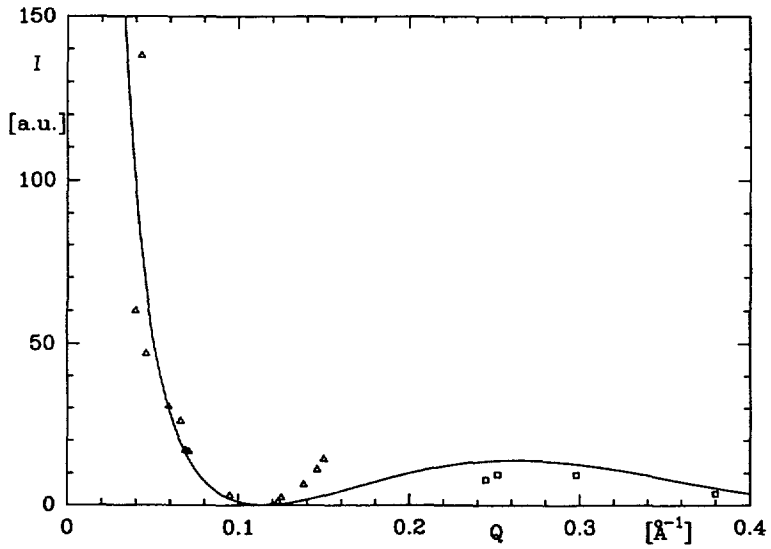

Fig. 4. — Normalized heights of the first and second order Bragg peaks as a function of their position in the X-ray experiment on AOT ; triangles : first order Bragg peak ; squares : second order Bragg peak ; the line is a fit to the model, see text below.

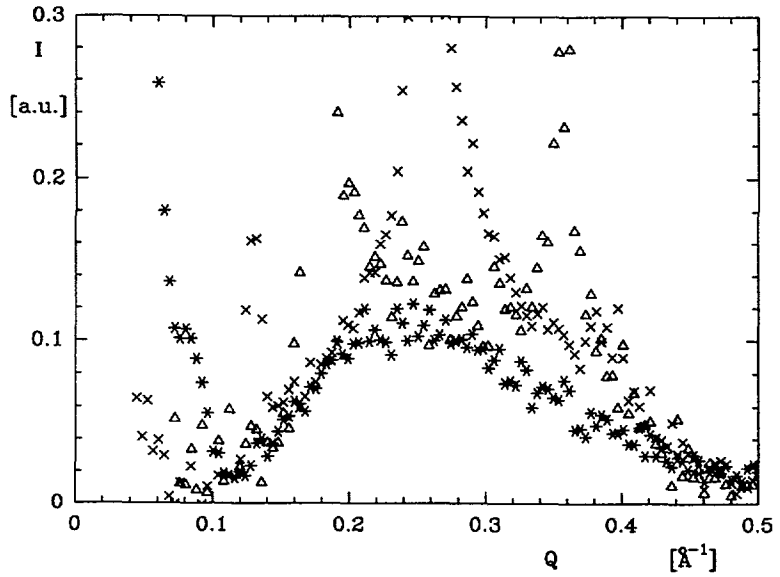

Fig. 5. — Diffuse part of the normalized intensity profiles in the X-ray scattering experiment on AOT ; the membrane volume fractions are, respectively : triangles 0.59, crosses 0.41, stars 0.14 ; the normalized diffuse scattering does not vary upon dilution of the lamellar phase.

order p is modulated by a factor $P(p \cdot q_0)$, where $P(q)$ is the form factor of the bilayer :

$$P(q) = \left| \int_0^{\delta} \rho_0(z)\, e^{iqz}\, dz \right|^2 \tag{3}$$

This property is at the very basis of a method widely used for inferring structural information about amphiphilic bilayers, which relies on the analysis of as many as possible Bragg peak intensities [4, 5].

However, the purely geometric model obviously fails for describing those features of the scattering spectrum that are related to thermal fluctuations. These features are the *shape* of the Bragg peaks and the occurrence of an *anisotropic small angle* scattering, as is now classically known, and also, as we show below, the occurrence of a *diffuse* scattering at large angles.

THERMODYNAMICAL MODELS. — Thermally-induced lattice vibrations have well-known consequences in the scattering spectra of *solids* : the peak heights are reduced by a Debye-Waller factor and some thermal-diffuse scattering arises at the base of Bragg peaks, which nevertheless keep their delta-function shapes [14]. For systems with smectic A order, with only *one* solid-like direction in 3D space, thermal motions have much more drastic consequences : first, the singularities at the Bragg positions become *weaker* than delta-functions [15, 16] and second, an anisotropic small angle scattering, much more intense along the z-axis than along the perpendicular directions arises [17, 18]. The Caillé model [15], taking into account properly the thermodynamics of a smectic A phase, describes rigorously these two features. Caillé chooses a scattering length density of the following form :

$$\rho(\mathbf{x}) \propto \sum_n \delta \left\{ z - nd + u_n(\mathbf{x}_\perp) \right\} \tag{4}$$

where $u_n(\mathbf{x}_\perp)$, displacement along z of the n-th layer at the transverse position $\mathbf{x}_\perp$, has Gaussian fluctuations according to the harmonic elastic theory of smectic A phases [19]. The model gives a very satisfactory account for the scattering profiles close to the Bragg positions [20-22], and of the small angle scattering [18, 23]. Owing to its description of a lamellar phase in terms of featureless, zero-thickness bilayers it nevertheless fails in explaining the form factor peak height modulation and the contrast-specific large angle diffuse scattering.

COMBINING GEOMETRY WITH THERMODYNAMICS. — It is unfortunately not easy to devise a model combining the relevant features of the previous two models, i.e. taking into account consistently both the geometry — the finite thickness of the membrane — and the thermodynamics — the layer displacement fluctuations. As a first step towards a complete rigorous theory, we introduce some kind of layer displacement fluctuations into the geometrical model in the following way : we assume that the n-th layer may fluctuate about its equilibrium position $n \,.\, d$ by an amount u_n *independent* of the transverse coordinates. This amounts to assuming that there is only compression and no curvature strains in the smectic phase. On the other hand, we assume that the u_n are Gaussian variables with the correlation function $\langle (u_n - u_0)^2 \rangle$ identical to the true smectic correlation function $\langle [u(\mathbf{x}_\perp = \mathbf{0}, z = n \,.\, d) - u(\mathbf{0}, 0)]^2 \rangle$, i.e. [15] :

$$\begin{aligned} \langle (u_n - u_0)^2 \rangle &= \frac{\eta n^2 d^2}{8}, \; n \text{ small} \\ \langle (u_n - u_0)^2 \rangle &= \frac{\eta}{2\pi^2} [\ln(\pi n) + \gamma] d^2, \quad n \gg 1 \end{aligned} \tag{5}$$

with γ Euler's constant and η defined in terms of the elastic constants of the smectic phase $\bar{B}$ and K by [15] :

$$\eta = \frac{q_0^2 k_B T}{8 \pi \sqrt{K \bar{B}}}. \tag{6}$$

With this amendment to the geometrical model, the scattering length density $\rho(\mathbf{x})$ becomes :

$$\rho(\mathbf{x}) = \sum_{0}^{N-1} \rho_0(z - nd + u_n), \quad |\mathbf{x}_\perp| < L_\perp$$
$$\rho(\mathbf{x}) = 0, \quad \text{otherwise}. \tag{7}$$

Substituting equation (7) into equation (1) leads to the following form for the intensity scattered by one isolated, finite-size crystal :

$$I_{id}(\mathbf{q}) = N \cdot P_\perp(\mathbf{q}_\perp) \cdot P(q_z) \cdot S(q_z) \tag{8}$$

where P is the form factor of the bilayer, equation (3), S is the normalized structure factor of the stack :

$$S(q_z) = 1 + 2 \sum_{1}^{N-1} \left(1 - \frac{n}{N}\right) \cos(nq_z d)\, e^{-\frac{q_z^2}{2}\langle (u_n - u_0)^2 \rangle} \tag{9}$$

and $P_\perp(\mathbf{q}_\perp)$ accounts for the finite transverse size of the bilayers. Its exact expression depends on the shape of the plaquettes, with the following general properties : $P_\perp$ is sharply peaked at $\mathbf{q}_\perp = \mathbf{0}$, with $P_\perp(\mathbf{0}) = L_\perp^4$; its width is of the order $2\pi/L_\perp$. It should be noted that our expression for the structure factor, equation (9), differs from those that result from « stacking disorder » of the first or second kind [6] (or, equivalently, for « perturbed regular lattices » or « paracrystalline lattices » [7]).

ACCOUNTING FOR FINITE RESOLUTION AND POWDER AVERAGING. — The above-described model gives a satisfactory, quantitative account for both our neutron and X-ray scattering data once powder averaging and finite instrumental resolution are considered. Finite resolution amounts to replacing the « ideal » intensity $I_{id}(\mathbf{q})$, equation (8), by the real one :

$$\tilde{I}(\mathbf{q}) = \int I_{id}(\mathbf{q}')\, R(\mathbf{q} - \mathbf{q}')\, d^3q' \tag{10}$$

where the resolution function $R(\mathbf{q})$ is chosen for convenience as a Gaussian profile of width Δq :

$$R(\mathbf{q}) = (2\pi\, \Delta q^2)^{-3/2} \exp\left(-\frac{q^2}{2\, \Delta q^2}\right). \tag{11}$$

For a crystal large enough, i.e. $L_\perp \Delta q \gg 1$ and $Nd\, \Delta q \gg 1$, the convolution, equation (10), is easily performed. Since $P_\perp$ is more sharply peaked than the resolution function, it may be represented by a delta-function :

$$P_\perp(\mathbf{q}_\perp) \cong 4\pi^2 L_\perp^2\, \delta(\mathbf{q}_\perp) \tag{12}$$

therefore leading, through convolution on $\mathbf{q}_\perp$ variables, to :

$$\tilde{P}_\perp(q_\perp) = 2\pi \frac{L_\perp^2}{\Delta q^2} \exp\left(-\frac{q_\perp^2}{2\, \Delta q^2}\right). \tag{13}$$

Along the q_z direction, using the fact that the membrane form factor $P(q_z)$ is a slowly varying function whereas the structure factor $S(q_z)$, sharply peaked, has much stronger variations, we approximate the effect of a finite resolution by convoluting the structure factor *alone*. This

yields the following expression for the resolution-limited structure factor :

$$\tilde{S}(q_z) = 1 + 2 \sum_{1}^{N-1} \left(1 - \frac{n}{N}\right) \cos\left(\frac{q_z\, dn}{1 + 2\,\Delta q^2\, d^2\, \alpha(n)}\right) \times \\ \times e^{-\frac{2\, q_z^2\, d^2 \alpha(n) + \Delta q^2\, d^2\, n^2}{2(1 + 2\,\Delta q^2\, d^2 \alpha(n))}} \frac{1}{\sqrt{1 + 2\,\Delta q^2\, d^2 \alpha(n)}} \quad (14)$$

where $\alpha(n)$ denotes the correlation function $\langle (u_n - u_0)^2 \rangle / 2\, d^2$.

The effects of thermal fluctuations on $\tilde{S}$ are illustrated in figure 6, which display the resolution-limited structure factor for $\eta = 0$ (no thermal fluctuations) and for η having non-zero values. The 0 K structure factor has identical peaks at each Bragg position, all with the same height of order $q_0/\sqrt{2\,\pi\,\Delta q}$, and negligible values (of order $1/N$) in-between peaks. In the presence of thermal fluctuations, higher order Bragg peaks are smoothed out (the third order peak almost disappears when η is increased from 0.1 to 0.2, for the example illustrated in Fig. 6) and a significant intensity, which reaches quickly its asymptotic value 1 appears *between* the peaks. Such a behaviour would be common for *disordered* systems as liquids. It illustrates here the dramatic effect of the Landau-Peierls instability in (ordered) systems with the smectic A symmetry. Note that the values we have chosen for η are realistic for lamellar systems stabilized by an electrostatic repulsion between bilayers, but that much larger values, close to $\eta = 1.3$ for large smectic spacings, are to be expected in many cases [21, 22].

For a random orientation of the crystal, it remains to powder-average the resolution-limited

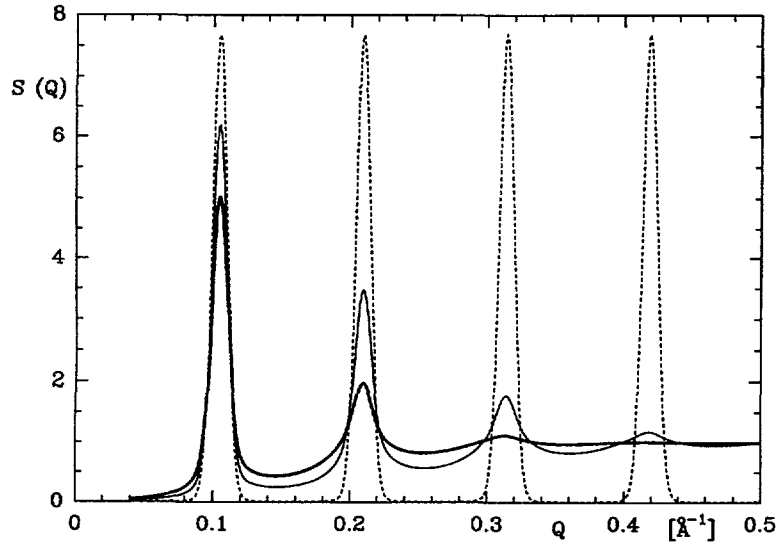

Fig. 6. — Structure factor of a $d = 60$ Å lamellar phase with some layer displacement fluctuations ; dotted curve : $\eta = 0$; continuous curve : $\eta = 0.1$; heavy line : $\eta = 0.2$; the latter values of η are typical for lamellar phases stabilized with either weakly screened electrostatic interactions or undulation interactions [22] ; the number of correlated layers in the stack is $N = 60$ and a finite resolution $\Delta q = 5.2 \times 10^{-3}$ Å^{-1} has been taken into account ; note how quickly the function reaches its asymptotic value 1 when $\eta \neq 0$.

intensity $\tilde{I}(\mathbf{q})$ according to :

$$I_{\text{powd}}(q) = N \int_0^1 \tilde{P}_\perp (\sqrt{1-x^2}\, q)\, P(qx)\, \tilde{S}(qx)\, \mathrm{d}x \,. \tag{15}$$

For large enough scattering wave vectors ($q \gg \Delta q$), $\tilde{P}_\perp$ as a function of x may be described as a properly normalized delta-function $\delta(x)$ [24], with therefore the resulting expression :

$$I_{\text{powd}}(q) = 2\,\pi\, \frac{N L_\perp^2}{q^2}\, P(q)\, \tilde{S}(q) \,. \tag{16}$$

Thus, the experimentally-recorded intensity scattered by an irradiated volume V containing $V/N d L_\perp^2$ finite-size crystals randomly oriented is finally given by :

$$I_{\text{exp}}(q) = 2\,\pi\, \frac{V}{d}\, \frac{P(q)\, \tilde{S}(q)}{q^2} \tag{17}$$

We have checked by a numerical evaluation of $\tilde{S}(q)$, equation (9), that our model, which clearly recovers a form factor peak height modulation, also yields power-law singularities in the vicinity of Bragg peaks. We got $\tilde{S}(q) \propto |q - q_0|^{-X}$, with an exponent X numerically close to $1 - \eta$. This is different from the Caillé result along the z-direction, namely $S_{\text{Caillé}}(q_z, \mathbf{q}_\perp = 0) \propto |q_z - q_0|^{-2+\eta}$ [15] ; our result is nevertheless correct for *powder* spectra, since the isotropically-averaged Caillé structure factor $\langle S_{\text{Caillé}} \rangle$ yields : $\langle S_{\text{Caillé}} \rangle (q) \propto |q - q_0|^{-1+\eta}$ [21, 22]. The value for η entering our model is therefore expected to be the true one, defined in terms of the elastic constants of the smectic liquid crystal, equation (6).

Our result incorporates a new feature, i.e. the appearance of a *diffuse scattering* at large wave vectors, controlled by the bilayer form factor, when the structure factor $\tilde{S}(q)$ reaches its asymptotic value 1. As exemplified in figure 6, this occurs in practice very soon. As already noticed [9], the diffuse scattering is experimentally identical, in absolute units, for lamellar (smectic A) and « sponge » (isotropic liquid) phases built with the same bilayer. Indeed, for « sponge » phases the intensity scattered by an irradiated volume V is given by [2, 3, 24] :

$$I_{\text{sponge}}(q) = 2\,\pi\, \frac{V\phi}{\delta}\, P(q)\, \frac{1}{q^2} \,. \tag{18}$$

Since the reticular distance d of a lamellar phase is related to bilayer thickness δ and volume fraction ϕ by the dilution law $d = \delta/\phi$, equation (17) and equation (18) are identical, apart from the lamellar phase structure factor.

NEUTRON AND X-RAY FORM FACTORS. — In order to compare our prediction, equation (17), with the X-ray and neutron scattering data we have taken simplified models for the scattering length density profile $\rho_0(z)$ of bilayers. For neutron scattering experiments on AOT/D_2O or DDAB/D_2O lamellar phases, a reasonable model is the square profile : $\rho_0(z) = \Delta\rho$, $0 \leqslant z \leqslant \delta$, where $\Delta\rho$ is the contrast between the hydrophobic part of the bilayer (of thickness δ) and the solvent (including the hydrated part of the bilayer ; see Fig. 7a). From equation (3), one then gets :

$$P_{\text{neut}}(q) = \frac{4}{q^2}\, \Delta\rho^2 \sin^2\left(q\,\frac{\delta}{2}\right) \,. \tag{19}$$

In practice, as apparent below, since the scattered intensity is not *truly* zero at the *large* wave vector $2\pi/\delta$, instead of equation (19) we use :

$$P_{\text{neut}}(q) = \frac{2\,\Delta\rho^2}{q^2}\,[1 - \cos\,(q\delta)\,e^{-q^2\sigma^2/2}] \qquad (19\text{bis})$$

with σ arbitrarily fixed at $\delta/4$; equation (19bis) may be viewed as the result of an averaging of equation (19) over a Gaussian distribution for δ, with width σ.

For X-ray scattering experiments, the profile $\rho_0(z)$ arises from the electron density distribution across the bilayer. The reasonable model is now a *two-square* profile, as sketched in figure 7b, because the electronic density of the hydrated polar heads in neither close to the electronic density of the solvent nor to that of the hydrophobic tails. We therefore take : $\rho_0(z) = \Delta\rho_H$ for $0 \leqslant z \leqslant \delta_H$ or $(\delta_H + 2\,\delta_T) \leqslant z \leqslant 2\,(\delta_H + \delta_T)$ and $\rho_0(z) = \Delta\rho_T$ for $\delta_H \leqslant z \leqslant (\delta_H + 2\,\delta_T)$. With these conventions the « scattering thickness » of the bilayer is $2(\delta_H + \delta_T)$. This form leads to :

$$P_{\text{X-ray}}(q) = \frac{4}{q^2}\,\{\Delta\rho_H[\sin\,[q(\delta_H + \delta_T)] - \sin\,(q\,\delta_T)] + \Delta\rho_T \sin\,(q\,\delta_T)\}^2 \qquad (20)$$

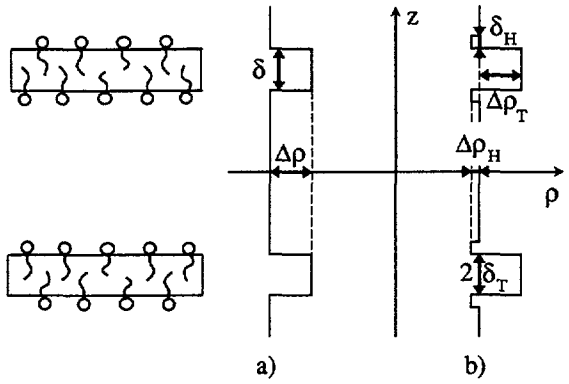

Fig. 7. — Schematic scattering length density profiles ρ_0 along the normal to the bilayer z ; a) neutron scattering experiment ; b) X-ray scattering experiment.

At contrast with the neutron form factor, equation (19), the X-ray form factor may have a zero for a wave vector q^* much *smaller* [25] than the reciprocal of the bilayer thickness (this occurs for instance at $q^* = 0.12$ Å^{-1} for $\Delta\rho_T/\Delta\rho_H = -0.16$, $\delta_H = 2.4$ Å and $\delta_T = 8.2$ Å). In such a case, the first order Bragg peak is removed from the observed X-ray spectrum at some point on the dilution line, as it is indeed observed on the AOT/H_2O system.

COMPARISON WITH EXPERIMENTAL DATA. — For neutron spectra, we have determined the relevant parameters — η and δ — by the following procedures : we get the two parameters, for each spectrum of the AOT/D_2O system, by fitting to the data either q^4 times the predicted intensity (Eq. (17)) or its logarithm. The first choice amounts to giving more weight to the high wave vector part of the spectrum, the second to its high intensity part. The two procedures give equivalent results for the parameter η, in the range 0.25, with a large uncertainty (about 40 %) and no significant variations along the dilution line, whereas the q^4-weighted procedure is definitely better, as might be expected, for the parameter δ. The bilayer thickness is constant

all along the dilution line (δ = 16 Å, with about 5 % uncertainty). Representative fits are displayed in figures 8a and 9a, for the ϕ = 0.20 sample ; all our other results have a similar quality. For the DDAB/D_2O samples, the q^4-weighted procedure is not very sensitive to η, nor the log-weighted one to δ. We therefore get first the parameter δ through the q^4-weighted procedure, which yields $\delta = 24.5 \pm 0.5$ Å for all our samples (Fig. 8b) (to be compared with δ = 24 Å in Ref. [10]). Then, keeping constant the bilayer thickness, we determine η with log-weighted data (Fig. 9b) ; we get η in the range 0.15. The values for η on both systems, though not very precise, are nevertheless nicely compatible with the ones expected for dilute lamellar phases stabilized by a weakly screened electrostatic repulsion

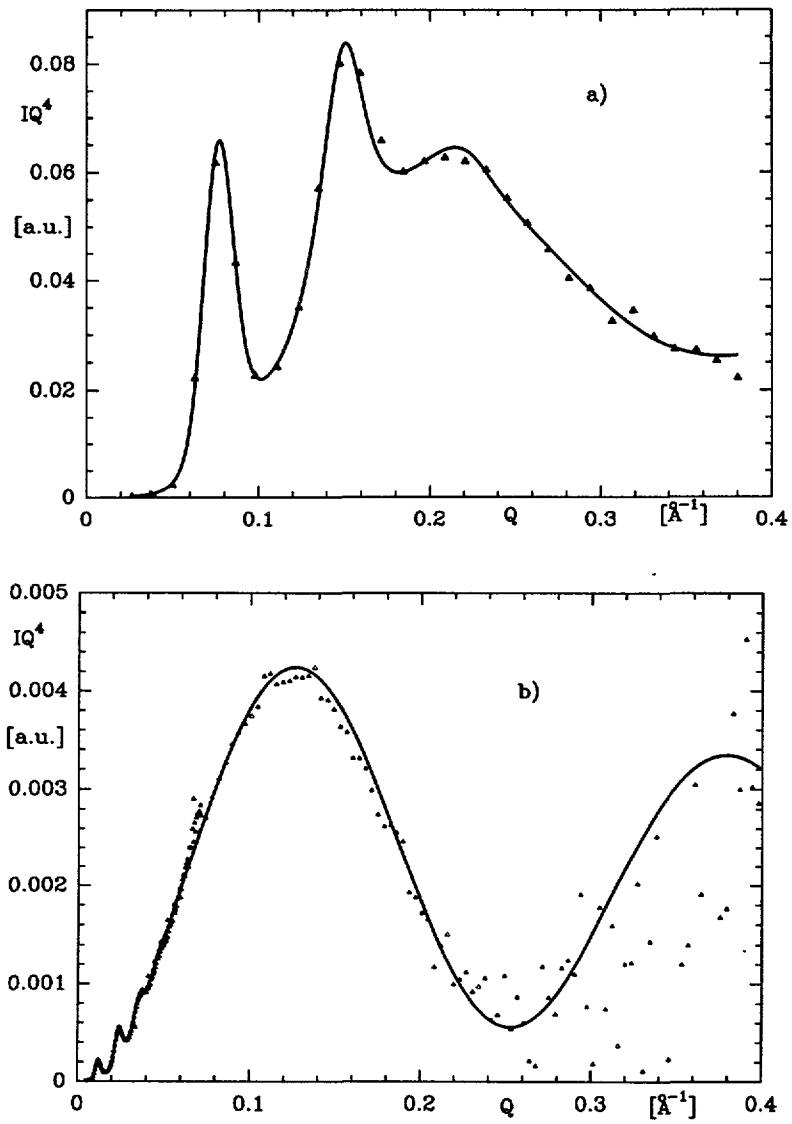

Fig. 8. — Selected examples of q^4 times the neutron intensity profiles, with fits to equation (17) ; a) AOT/D_2O system at ϕ = 0.20 ; the bilayer thickness is δ = 16 Å ; b) DDAB/D_2O system at ϕ = 0.04 ; the bilayer thickness is δ = 24.5 Å.

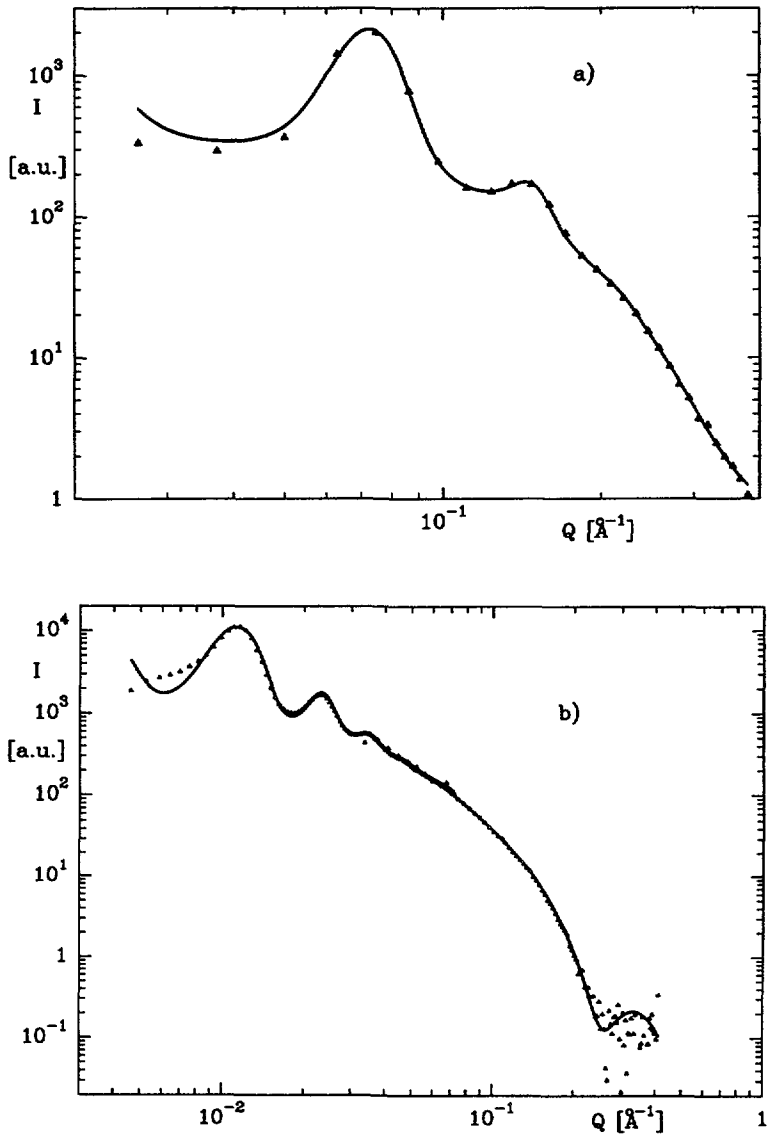

Fig. 9. — Selected examples of the neutron intensity profiles, with fits to equation (17) ; a) AOT/D_2O system at $\phi = 0.20$; $\eta = 0.25$; b) DDAB/D_2O system at $\phi = 0.04$; $\eta = 0.16$.

between bilayers [22]. For all the fits, the other parameters entering equation (17) are either fixed to measured values or irrelevant : the smectic period d is deduced from the peak position ; the width Δq of the resolution function, equation (11), is $\Delta q = 1.8 \times 10^{-3}$ Å^{-1} on PAXY (DDAB experiment) or $\Delta q = 8 \times 10^{-3}$ Å^{-1} on PAXE (AOT experiment) ; the number of correlated layers N (Eqs. (9) or (14)) has no influence as soon as the peaks in $S(q)$, equation (9), have a width smaller than Δq, which occurs for N greater than about $q_0/\Delta q$.

For X-ray spectra, four parameters have to be determined. Since there is neither large intensity nor wave vector differences between the form and structure factor contributions to the

scattered intensity, especially at dilutions around $\phi = 40\ \%$, we have not tried to extract all four parameters on each spectrum. Instead, we first determine the three parameters describing the form factor of the bilayer, equation (20), by fitting to the theoretical expression equation (17) the *large wave vector part* ($q > 0.1\ \text{Å}^{-1}$) of the intensity scattered by a *dilute* AOT sample ($\phi < 0.25$), assuming that in this large q range the structure factor has reached its asymptotic value, $\tilde{S}(q \gg q_0) = 1$. The fitted parameters are : $\delta_H = 2.4\ \text{Å}$, $\delta_T = 8.2\ \text{Å}$ and $\Delta\rho_T/\Delta\rho_H = -0.16$. Then, in a second step, we have fitted for each AOT sample the whole q range to equation (17), with the previously determined bilayer form factor parameters kept constant and now only *one* relevant fitting parameter, η (the width of the resolution function is here fixed to $\Delta q = 5.2 \times 10^{-3}\ \text{Å}^{-1}$). As it is clear from the two examples displayed in figure 10, the model, equation (17), describes also well the X-ray data, in particular those with small intensity Bragg peaks. It should nevertheless be mentioned that the values we get for the exponent η, about 0.15, are definitely smaller than those extracted from the neutron data on the same system [26] ; they are still in a reasonable range.

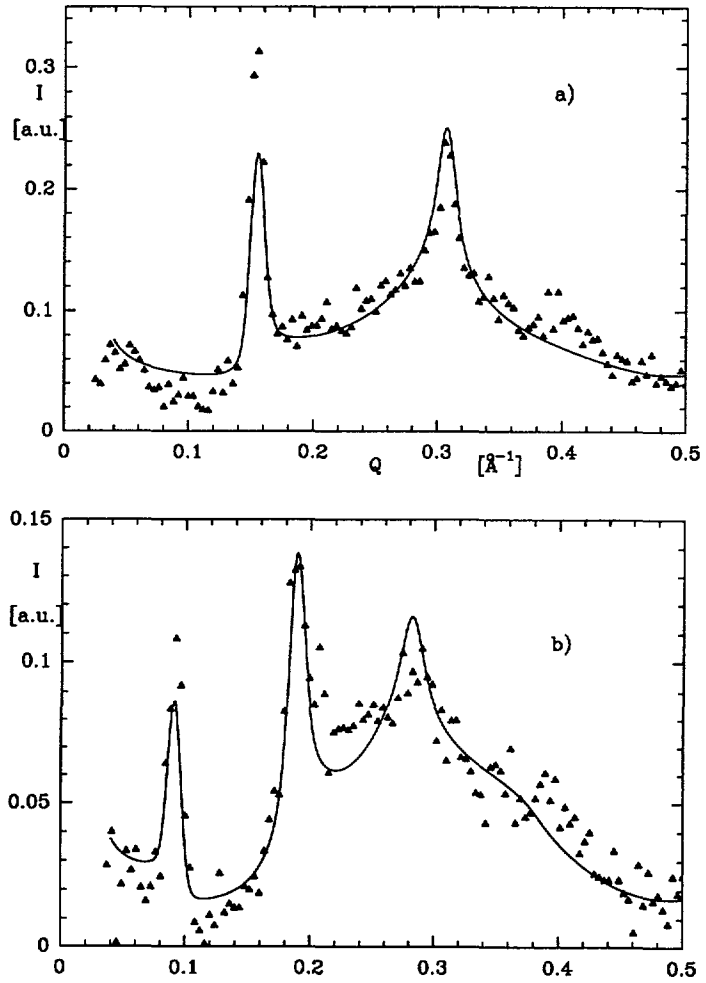

Fig. 10. — Selected examples of the X-ray intensity profiles (AOT/H_2O system) fitted to equation (17) ; a) $\phi = 0.48$ with $\eta = 0.18$; b) $\phi = 0.28$ with $\eta = 0.13$.

The fitted form factor, equation (20), with the $1/q^2$ normalization arising from powder averaging, is superimposed to the X-ray peak height data in figure 4, showing a peak height modulation. The X-ray parameters δ_H and δ_T correspond to an apparent thickness for the bilayer of 21.2 Å, in good agreement with the geometrical value (21 Å ; 19.5 Å in Ref. [12]) deduced from the variation of q_0 with composition. The neutron result $\delta = 16$ Å, corresponding to the thickness of the *hydrophobic core* of the bilayer, is consistently smaller than the X-ray value.

In spite of the various approximations that led to equation (17), it appears that the quantitative description of the scattered intensity it gives, on the basis of a model that takes into account both the geometry of the bilayers (membrane form factor) and the thermodynamics of the smectic phase (layer displacement fluctuations) is essentially valid both near or at the peaks and at large angles. More effort is to be exercised yet in order to get *precise* values for the elastic parameter η. Nevertheless, the physical meaning of this parameter is clear : it would not have been possible, for instance, to describe even semi-quantitatively the spectra by imposing $\eta = 0$ (no thermal fluctuations) from the start.

Conclusion.

X-ray and neutron scattering experiments have been performed on various lamellar phase samples in the AOT/water and DDAB/water systems, along dilution lines. We show that the large wave vectors features of the scattering spectra have the same origin in these smectic A phases as it is classically known in liquid phases, namely the form factor of the building objects. The physical origin for such a behaviour lies in the long wavelength, thermally excited elastic fluctuations of the crystalline structure : owing to the Landau-Peierls instability, the structure factor reaches quickly 1, its asymptotic value. Some care should therefore be exercised in inferring form factor parameters from peak height analyses only. The simple model that we propose, combining the geometry of the bilayer with thermal layer displacement fluctuations provides a general and quite elegant method for studying both form factors and elastic properties of lamellar phases. Its remarkable ability in describing scattering data is an illustration of this viewpoint.

Acknowledgments.

U. Olsson aroused our initial interest for the scattering properties of the AOT/water system. The kind hospitality of J. Teixera at Laboratoire Léon-Brillouin is gratefully acknowledged. We warmly thank C. R. Safinya, for very kindly introducing us to the arcana of thermal-diffuse scattering. It is a real pleasure to thank Thomas N. Zemb, whose pertinent advice and keen comments on many aspects of this work were of considerable value.

References

[1] EKWALL P., Advances in Liquid Crystals, G. M. Brown Ed. (Academic Press, New York, 1975).
[2] PORTE G., MARIGNAN J., BASSEREAU P. and MAY R., *J. Phys. France* **49** (1988) 511.
[3] GAZEAU D., BELLOCQ A.-M., ROUX D. and ZEMB Th., *Europhys. Lett.* **9** (1989) 447.
[4] LUZZATI V., Biological Membranes, D. Chapman Ed. (Academic Press, New York, 1967).
[5] MARIANI P., LUZZATI V. and DELACROIX H., *J. Mol. Biol.* **204** (1988) 165.
[6] BLAUROCK A. E., *Biochim. Biophys. Acta* **650** (1982) 167.
[7] WELBERRY T. R., *Rep. Prog. Phys.* **48** (1985) 1543.
[8] RANÇON Y. and CHARVOLIN J., *J. Phys. France* **48** (1987) 1067 ;
CLERC M., LEVELUT A.-M. and SADOC J.-F., *J. Phys. II France* **1** (1991) 1263.

[9] SKOURI M., MARIGNAN J. and MAY R., *Colloid Polym. Sci.* **269** (1991) 929.
[10] DUBOIS M. and ZEMB Th.. *Langmuir* **7** (1991) 1352 ;
DUBOIS M., thèse (université Paris-XI, 1991).
[11] ROGERS J. and WINSOR P. A., *Nature* **216** (1967) 477.
[12] FONTELL K., *J. Colloid Interface Sci.* **44** (1973) 318.
[13] ROUX D., NALLET F., FREYSSINGEAS E., PORTE G., BASSEREAU P., SKOURI M. and MARIGNAN J., *Europhys. Lett.* **17** (1992) 575.
[14] E. g. : GUINIER A., Théorie et technique de la radiocristallographie (Dunod, Paris, 1964) ;
AZAROFF L. V., Elements of X-Ray Crystallography (McGraw-Hill, New York, 1968).
[15] CAILLÉ A., *C.R. Hebdo. Acad. Sci. Paris* **B 274** (1972) 891.
[16] GUNTHER L., IMRY Y. and LAJZEROWICZ J., *Phys. Rev.* **A 22** (1980) 1733.
[17] PORTE G., MARIGNAN J., BASSEREAU P. and MAY R., *Europhys. Lett.* **7** (1988) 713.
[18] NALLET F., ROUX D. and MILNER S. T., *J. Phys. France* **51** (1990) 2333.
[19] DE GENNES P.-G., *J. Phys. Colloq. France* **30** (1969) C4-65.
[20] ALS-NIELSEN J., LITSTER J. D., BIRGENAU D., KAPLAN M., SAFINYA C. R., LINDGAARD-ANDERSEN A. and MATHIESEN S., *Phys. Rev.* **B 22** (1980) 312.
[21] SAFINYA C. R., ROUX D., SMITH G. S., SINHA S. K., DIMON P., CLARK N. A. and BELLOCQ A.-M., *Phys. Rev. Lett.* **57** (1986) 2718.
[22] ROUX D. and SAFINYA C. R., *J. Phys. France* **49** (1988) 307 ;
SAFINYA C. R., SIROTA E. B., ROUX D. and SMITH G. S., *Phys. Rev. Lett.* **62** (1989) 1134.
[23] MILNER S. T., private communication.
[24] GLATTER O. and KRATKY O., Small Angle X-ray Scattering (Academic Press, New York, 1982).
[25] As in the neutron scattering case previously discussed, the X-ray scattered intensity is not exactly zero at q^* ; it is nevertheless *much smaller* than the surrounding intensities. There is thus no need to smooth the test function describing the X-ray form factor.
[26] Our somewhat approximate treatment of the resolution function in neutron scattering experiments (we have not taken into account the increase, owing to a finite $\Delta\lambda/\lambda$, in Δq with the scattering wave vector) could explain the differences between X-ray and neutron results for η on the same system.